OSU Oregon State UNIVERSITY

Open Access Articles

Control of Crystallographic Texture and Surface Morphology of Pt/TiO_2 Templates for Enhanced PZT Thin Film Texture

The Faculty of Oregon State University has made this article openly available.
Please share how this access benefits you. Your story matters.

Citation	Fox, A. J., Drawl, B., Fox, G. R., Gibbons, B. J., & Trolier-McKinstry, S. (2015). Control of Crystallographic Texture and Surface Morphology of Pt/TiO_2 Templates for Enhanced PZT Thin Film Texture. IEEE Transactions on Ultrasonics, Ferroelectrics, and Frequency Control, 62(1), 56-61. doi:10.1109/TUFFC.2014.006671
DOI	10.1109/TUFFC.2014.006671
Publisher	IEEE - Institute of Electrical and Electronics Engineers
Version	Accepted Manuscript
Terms of Use	http://cdss.library.oregonstate.edu/sa-termsofuse

Oregon State UNIVERSITY OSU

Control of Crystallographic Texture and Surface Morphology of Pt/TiO_2 Templates for Enhanced PZT Thin Film Texture

Austin J. Fox, *Member, IEEE*, Bill Drawl, Glen R. Fox, *Senior Member, IEEE*, Brady J. Gibbons, *Member, IEEE*, and Susan Trolier-McKinstry, *Fellow, IEEE*

Abstract*— Optimized processing conditions for $Pt/TiO_2/SiO_2/Si$ templating electrodes were investigated. These electrodes are used to obtain [111] textured thin film lead zirconate titanate ($Pb[Zr_xTi_{1-x}]O_3$ $0 \leq x \leq 1$) (PZT). Titanium deposited by dc magnetron sputtering yields [0001] texture on a thermally oxidized Si wafer. It was found that by optimizing deposition time, pressure, power, and the chamber pre-conditioning, the Ti texture could be maximized while maintaining low surface roughness. When oxidized, titanium yields [100] oriented rutile. This seed layer has as low as a 4.6% lattice mismatch with [111] Pt, thus it is possible to achieve strongly oriented [111] Pt. The quality of the orientation and surface roughness of the TiO_2 and the Ti directly affect the achievable Pt texture and surface morphology. A transition between optimal crystallographic texture and the smoothest templating surface occurs at approximately 30 nm of original Ti thickness (45 nm TiO_2). This corresponds to 0.5 nm (2 nm for TiO_2) RMS roughness as determined by atomic force microscopy and a FWHM of the rocking curve 0002 (200) peak of 5.5° (3.1° for TiO_2). A $Pb[Zr_{0.52}Ti_{0.48}]O_3$ layer was deposited and shown to template from the textured Pt electrode, with a maximum [111] Lotgering factor of 87% and a minimum 111 FWHM of 2.4° at approximately 30 nm of original Ti.

***Index Terms*— Crystallographic Orientation, Piezoelectric, Thin Films**

This paper was submitted on July 31st, 2014 for review. This research was partially sponsored by the Army Research Laboratory and was accomplished under Cooperative Agreement Number W911NF-11-2-0053, the Penn State National Nanotechnology Infrastructure Network (NNIN) node supported by the National Science Foundation, the Oregon State University Graduate School Provost's Fellowship, and the NSF CAREER Award, grant No. DMR 115170.

Austin J. Fox is with Materials Science, School of Mechanical, Industrial, and Manufacturing Engineering at Oregon State University, Corvallis, OR 97330 USA (e-mail: foxa@onid.orst.edu).

Bill Drawl is with the Materials Research Institute at Penn State University, State College, PA 16802 USA (e-mail: wrd1@psu.edu).

Glen R. Fox is with Fox Materials Consulting LLC, Colorado Springs, CO 80908 USA (e-mail: glen_fox_pa@msn.com).

Brady J. Gibbons is with Materials Science, School of Mechanical, Industrial, and Manufacturing Engineering at Oregon State University, Corvallis, OR 97330 USA (e-mail: brady.gibbons@oregonstate.edu).

Susan Trolier-McKinstry is with the Materials Research Institute at Penn State University, State College, PA 16802 USA (e-mail: STMcKinstry@psu.edu).

I. Introduction

Material properties, e.g. conductivity, piezoelectricity, and ferromagnetism, exhibit the anisotropy of the atomic structure [1]. Thus, it is crucial to understand the development and control of crystallographic texture to achieve high device response, efficiency, and reliability. In thin film embodiments, many deposition methods allow for achieving uniaxial fiber texture, where columnar grains grow with a particular crystal direction parallel to the normal of the substrate surface. Texture development in thin films is driven by many factors. Films grown at relatively high temperatures on smooth amorphous or polycrystalline substrates tend to orient such that the lowest surface-energy crystal plane is parallel to the substrate surface (typically this would be the closest-packed plane). At lower temperatures where adatom surface diffusion is limited, the planes that grow or nucleate the fastest drive the texture development. Films grown on smooth, crystallographically textured polycrystalline substrates with a lattice parameter similar to the underlying material will typically template and mimic the orientation of this substrate. This is also known as granular epitaxy and results in fiber texture [2].

For both amorphous and polycrystalline substrates, when the surface tension of the substrate/film plus film/ambient interfaces is greater than the substrate/ambient interface, growth is expected to follow Volmer-Weber mode (island growth) [2]. In this mode islands nucleate and grow, coalescing and forming grains that grow in a columnar fashion. Some of these columnar grains will grow faster than others, eventually resulting in surface roughness and/or coning over other grains. It is expected that a relatively high degree of substrate surface roughness will limit the achievable texture of the overlying deposited film.

SiO_2/Si is used as a smooth surface on which to grow high quality electrodes and subsequently ferroelectric and piezoelectric devices [3], [4]. It is important that the electrode (most often Pt) adheres well to the substrate (SiO_2/Si), has minimal interdiffusion pathways, and has high conductivity [3], [5]. In the case of PZT, if the electrode is susceptible to Pb diffusion, the Pb will react with SiO_2 to form $PbSiO_3$ [6]. This in turn disrupts the SiO_2 insulation properties and leaves the PZT Pb deficient [7]. To minimize diffusion pathways,

electrode density must be maximized. A robust and reproducible interface results from control over underlying surface morphology and the presence of a good lattice match between the electrode and PZT. High density, surface smoothness, and texture can be achieved by sputter depositing fiber textured Pt under optimized conditions.

In this study, an initial seed layer, hexagonal close packed (HCP) Ti, is grown on an amorphous and nearly atomically smooth SiO_2 layer. Ti grows via Volmer-Weber mode from the HCP basal plane, leading to [0001] fiber texture. Oxidation of the Ti is then used to obtain TiO_2 in the rutile phase with a [100] fiber texture. Rutile (001) has a lattice match, at room temperature, with Pt (111). Specifically, Pt <110> has a mismatch of 6.2% with rutile <001> and Pt <112> has a mismatch of 4.6% with rutile <010>. For templating to occur, a mismatch of less than 15% is typically necessary [8].

Here the effect of coning and surface roughness as a function of thickness of initial Ti is used to look at the growth characteristics of sputtered Ti, as well as the surface roughness effect on texture and roughness development of the Pt overlying film. The intermediate stage of oxidation is also analyzed to determine its effect on the crystal lattice, thickness, and surface morphology. As proof of concept, a $Pb[Zr_{0.52}Ti_{0.48}]O_3$ (PZT(52/48)) layer was deposited and shown to template from the Pt.

II. Experimental Procedure

Wafers of [100]-oriented silicon with 500 nm thermally grown silica were diced into 1 inch by 1 inch sections. Diced wafers were ultrasonically cleaned for 5 minutes successively in solutions of acetone, methanol, and isopropyl alcohol and were dried with flowing N_2 after each submersion. Subsequently, Ti was deposited by dc magnetron sputtering from a 99.99% pure Ti target. The Ti films were then thermally oxidized, and a Pt layer was deposited by dc magnetron sputtering from a 99.99% pure Pt target, following the work by *Potrepka, et al.* [9]. Between each step, x-ray diffraction measurements (XRD, Bruker D8 Discover, Cu K_α) were taken to determine the extent of crystallographic texture. Atomic force microscopy (AFM, MFP-3D, Asylum Research) was used to determine surface roughness and morphology.

All depositions were completed in a Kurt J. Lesker CMS-18 in an argon atmosphere with 3 inch targets, a 15 cm throw distance, continuous rotation, and magnetron displacement of 15° from the substrate surface normal. For the titanium deposition, a chamber pre-conditioning was performed to ensure that the oxygen partial pressure was as low as possible. Oxygen solubility in Ti can be up to 33% in HCP interstitial sites, causing a shift in lattice parameters (see Fig. 1) [10]. It was observed that at base pressures above 1×10^{-7} Torr the degree of Ti texture (as measured by FWHM) was greatly limited. This could be due to these lattice parameter shifts, thus necessitating chamber pre-conditioning. The pre-conditioning was completed in an argon atmosphere at a pressure of 5 mTorr, a dc power of 200 W, and a 20 min sputtering time. The titanium film deposition was then performed at 200 W and 2 mTorr for 100, 200, 300, 500, 750, 1000, and 1500 s. All Ti depositions were completed at room temperature. A sputter rate of 1 Å/s was determined via profilometry (Tencor, Alpha-step IQ).

The Ti films were thermally oxidized using a Modular Process Technology Corporation rapid thermal processor - 600S. Temperature was ramped at 20 °C/s to 700 °C where they were held for 10 min and then cooled as quickly as possible. The entire cycle was completed under 10 SLPM of flowing O_2.

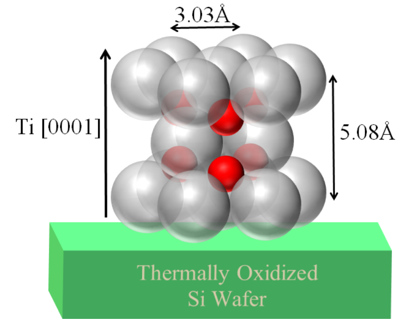

Fig. 1. The Ti HCP unit cell indicating where oxygen can incorporate and the effect on the lattice parameters. For Ti without any incorporated oxygen, a = 2.95 Å and c = 4.68 Å.

The thicknesses of the oxidized films were determined using spectroscopic ellipsometry (SE, J.A. Woolam, V-VASE). The layer was modeled using a Cauchy formalism for wavelengths from 400 nm – 1500 nm.

Pt was deposited on the oxidized Ti at 5 mTorr with a dc power of 200 W for 410 s, yielding approximately 110 nm. The substrate was heated to 600 °C for the deposition and was held for 30 min after the end of the deposition to anneal the film. This allows for structural rearrangement and relaxation. Ideally, this anneal enhances texture development and allows for grain growth and densification.

PZT(52/48) was deposited via chemical solution deposition (CSD) on the $Pt/TiO_2/SiO_2$ wafers. Solutions were prepared using the inverted mixing order (IMO) method [11].

In an atmosphere controlled glove box, B-site cation precursors (zirconium n-butoxide, 80% and titanium isopropoxide, 97%) were mixed and stirred for 5 min at room temperature. Acetic acid was then added and stirred for 5 min at room temperature to chelate the precursors. The solution was then diluted with methanol and again stirred for 5 min at room temperature. After removing from the glove box, lead (II) acetate trihydrate ($Pb(CH_3COO)_2 \cdot 3H_2O$) was added, dissolved at 90°C, and stirred for 20 min at temperature. 10 mol% excess Pb was added to account for Pb volatility during crystallization.

The solution was then stirred for a minimum of 30 min before spin casting at 3000 rpm for 30 s onto the $Pt/TiO_2/SiO_2$ substrates. Films were pyrolyzed at 300°C for 1 min after every layer. After every 4 layers, they were crystalized at 700°C for 10 min. A total of 8 layers were deposited to achieve film thicknesses of approximately 550 nm.

III. Results and Discussion

XRD patterns of a representative as-deposited Ti film reveal that only the 0002 and 0004 reflections of HCP Ti are observed, along with the substrate peaks (Fig. 2, top). This shows that the as-deposited Ti is strongly [0001] textured. To determine the extent of texture, XRD rocking-curves of the 0002 Ti peak were completed.

With increased Ti deposition time, the rocking-curves indicate that the resulting orientation is markedly improved (Fig. 3). The surface roughness, measured by AFM, also increases with increased deposition time (Fig. 4). These two results suggest that the Ti deposited under the conditions used in this work grows with fiber texture via the Volmer-Weber mode.

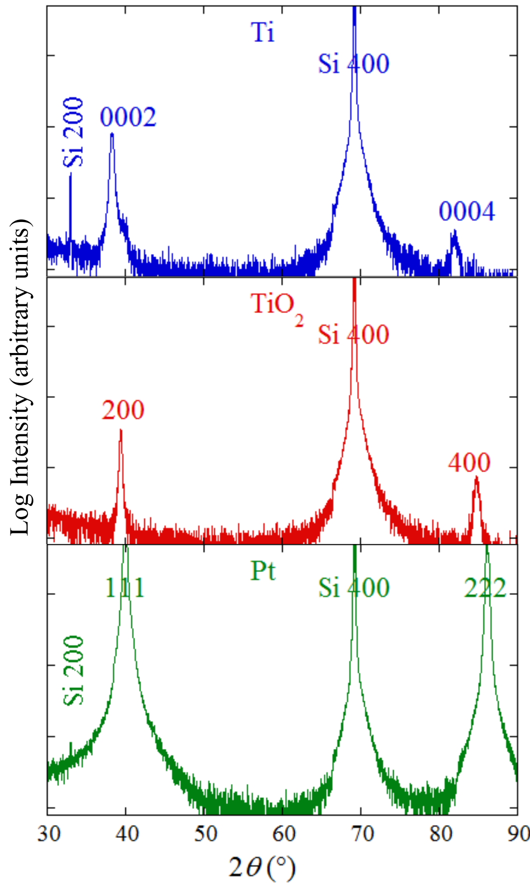

Fig. 2. Representative θ-2θ diffraction patterns.

The θ-2θ scans after oxidation show only the 200 and 400 TiO_2 rutile peaks (Fig. 2, middle), meaning the fiber texture is maintained through the phase transformation. The rocking-curve scans of the 200 peak show that the texture is actually improved (Fig. 5) for the TiO_2 in comparison with the starting Ti film. This is most likely due to some combination of lattice rearrangement caused by the elevated temperature and expansion of the lattice during oxidation. The oxidation induced thickness expansion is depicted in Fig. 6, where the SE determined TiO_2 thickness is plotted vs. the initial Ti thickness obtained by profilometry.

The Ti to TiO_2 phase transformation likely also has some impact on the surface roughness of the TiO_2 due to the volume expansion of the lattice. This expansion will cause stress in the structure that, when relieved, may slightly change the orientation of some grains. It was previously reported that oxidation resulted in subsequent adhesion loss in some cases, but for the work reported herein no signs of compressive delamination were observed [12]. The surface roughness of the rutile is increased from that of the Ti and has a distinct change in slope that is not apparent in the Ti curve starting at approximately 30 nm of starting Ti (Fig. 4). One possible explanation of this increase is that above 30 nm of initial Ti, stress induced rearrangement during oxidation begins to dominate, thus altering the structure and film morphology.

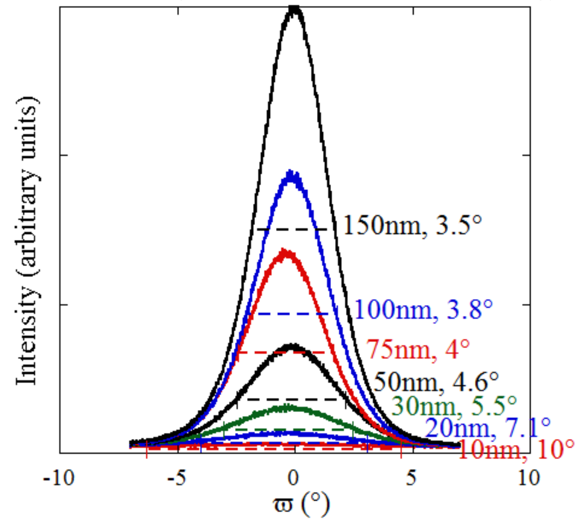

Fig. 3. Ti 0002 rocking curves.

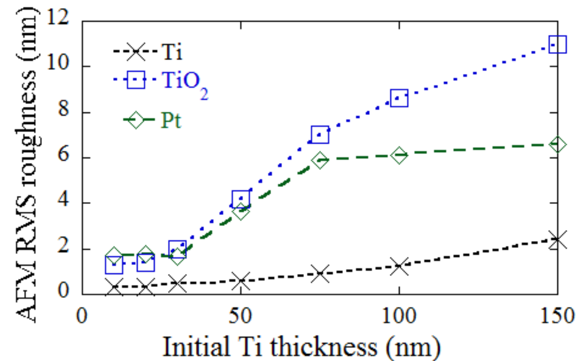

Fig. 4. Surface roughness of different layers vs. Ti thickness.

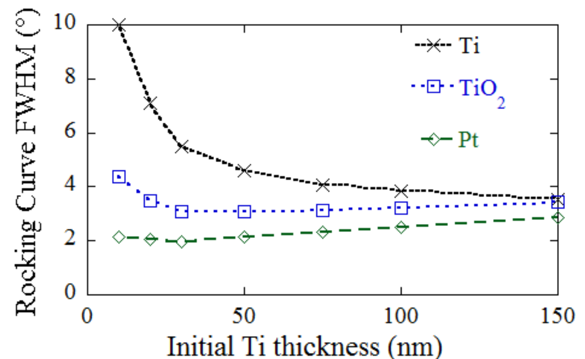

Fig. 5. Rocking curve comparison.

The Pt θ-2θ scans show a very high degree of [111] texture (Fig. 2, bottom). The rocking curves display a slight initial improvement in texture but the texture begins to degrade at ≈ 30 nm of initial Ti thickness (Fig. 5). The surface roughness also increases sharply at ≈ 30 nm (Fig. 4).

Initially, the texture of the Pt is controlled only by the texture of the underlying TiO_2 layer, but at ≈ 45 nm of TiO_2 (2 nm RMS surface roughness), the Pt texture begins to be limited by the roughness of the TiO_2.

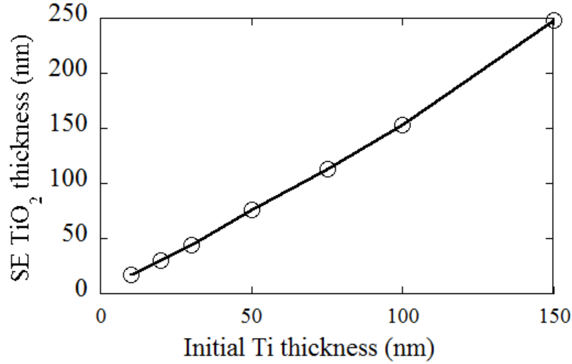

Fig. 6. SE TiO_2 thickness vs. Initial Ti thickness

Above 30 nm of initial Ti, the film is thick enough that the effect of coning is significant and the faster growing grains are overtaking the slower growing ones. This can be observed in the grain size variations observed via AFM (Fig. 7). The effect of grain size distribution on the roughness is exacerbated by the thermal oxidation that expands the lattice, forcing the grain surfaces upward. The Pt layer surface roughness follows that of the TiO_2 (Fig. 4) and the texture degrades above 30 nm of Ti due to the rougher TiO_2 surface (Fig. 5).

The θ-2θ diffraction patterns of PZT deposited on $Pt/TiO_2/SiO_2$ with different thicknesses of initial Ti are shown in Fig. 8. Based on these data, no second phases are observed and there is a degree of [111] texture, as indicated by the maxima at the 111 peaks. The degree of [111] PZT texture can be evaluated using the Lotgering factor, f (eq. 1), where p (eq. 2) is the ratio of the sum of the 111 and 222 peak intensities divided by the sum of all peak intensities (I) and p_o is for that of a randomly oriented sample [13].

$$f = \frac{p - p_o}{1 - p_o} \tag{1}$$

$$p = \frac{\sum I(111 + 222)}{\sum I(hkl)} \tag{2}$$

Fig. 9 shows the Lotgering factor versus initial Ti thickness. In this plot, a trend similar to that of the Pt FWHM is seen (although the film with 75 nm of initial Ti seems to fall out of the trend). The overall degree of texture is not as high when compared to films deposited by other groups and this is attributed to different PZT film preparation methods including incomplete optimization of composition and anneal conditions [9], [14].

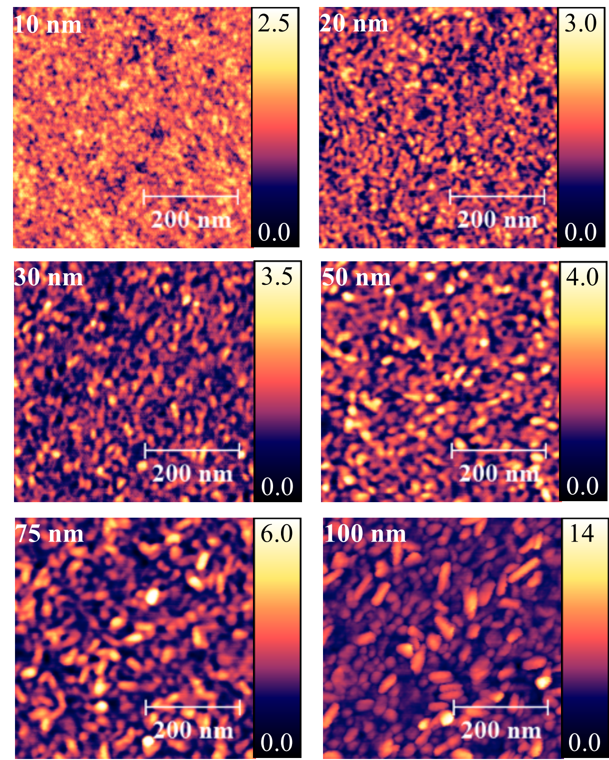

Fig. 7. AFM micrographs of as deposited Ti. False color scales are in nm.

The rocking curve scans (Fig. 10) of the PZT 222 peak show a similar trend to that of the Pt. The trend comparison can be seen in Fig. 11, where all layers are plotted. The consistency of the trends illustrates that PZT texture is very dependent on the texture and roughness of the underlying Pt substrate. It is difficult to say whether texture or roughness dominates without developing a method to decouple these two parameters in the Pt layer.

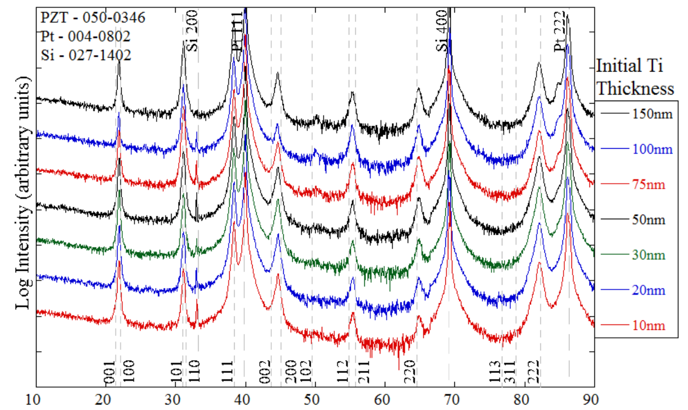

Fig. 8. PZT θ-2θ diffraction patterns, showing single phase [111] textured PZT.

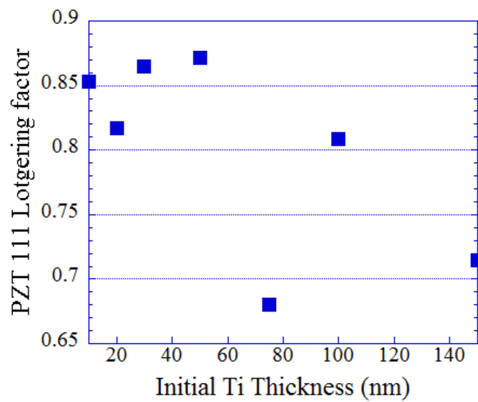

Fig. 9. PZT 111 Lotgering factors

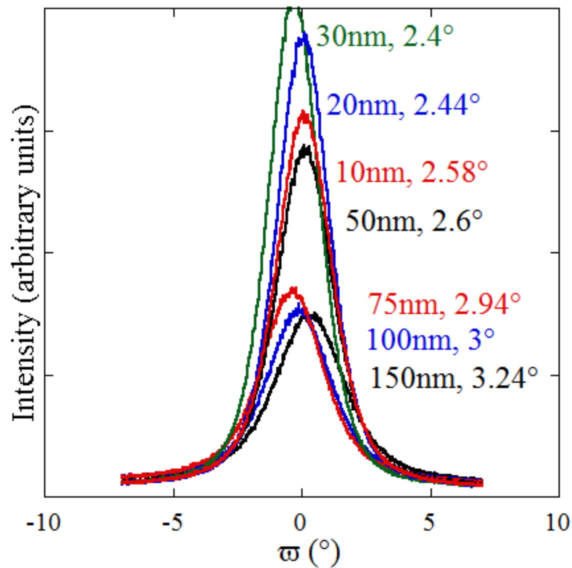

Fig. 10. PZT 222 rocking curves

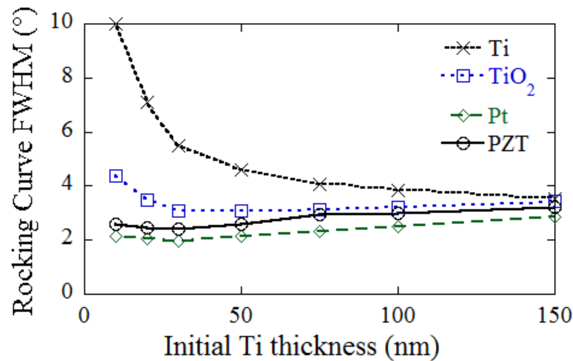

Fig. 11. Rocking curve comparison

IV. Conclusions

Data were presented to show that Pt thin film texture and surface roughness depend on the texture and surface roughness of the underlying TiO_2, which is in turn strongly dependent on the starting Ti. A roughness transition occurs at an initial Ti thickness of approximately 30 nm. A cross-sectional TEM study investigating the interfaces and the Ti/TiO_2 microstructure could help determine the source of the transition at 30 nm of Ti. PZT was also shown to template from textured Pt. No direct correlation between Pt roughness and texture and PZT texture could be deduced from the current study. A method to decouple surface roughness and crystal texture in Pt will need to be developed for further understanding.

V. References

[1] R. E. Newnham, *Properties of Materials*. Oxford University Press, 2005, p. 378.

[2] M. Ohring, *The Materials Science of Thin Films*. Academic Press, 1992, p. 704.

[3] G. R. Fox, S. Trolier-McKinstry, and S. B. Krupanidhi, “Pt/Ti/SiO_2/Si substrates,” *J. Mater. Res.*, vol. 10, no. 6, pp. 1508–1515, 1995.

[4] D. Newns, B. Elmegreen, X. Hu Liu, and G. Martyna, “A low-voltage high-speed electronic switch based on piezoelectric transduction,” *J. Appl. Phys.*, vol. 111, no. 8, p. 084509, 2012.

[5] K. Sreenivas, I. Reaney, T. Maeder, N. Setter, C. Jagadish, and R. G. Elliman, “Investigation of Pt / Ti bilayer metallization film integration on silicon for ferroelectric,” *J. Appl. Phys.*, vol. 75, no. 1, pp. 232–239, 1994.

[6] C. T. Shelton, P. G. Kotula, G. L. Brennecka, P. G. Lam, K. E. Meyer, J.-P. Maria, B. J. Gibbons, and J. F. Ihlefeld, “Chemically Homogeneous Complex Oxide Thin Films Via Improved Substrate Metallization,” *Adv. Funct. Mater.*, vol. 22, no. 11, pp. 2295–2302, Jun. 2012.

[7] R. A. Roy and K. F. Etzold, “Substrate and Temperature effects in Lead Zircconate Titonate Films Produced by Facing Targets Sputtering,” *J. Mater. Res.*, vol. 7, no. 6, pp. 1455–1464, Jun. 1992.

[8] M. A. Herman, W. Richter, and H. Sitter, *Epitaxy*. Springer, 2004, p. 507.

[9] D. M. Potrepka, G. R. Fox, L. M. Sanchez, and R. G. Polcawich, “Pt/TiO_2 Growth Templates for Enhanced PZT films and MEMS Devices,” *MRS Proc.*, vol. 1299, pp. 67–72, Jan. 2011.

[10] A. V. Ruban, V. I. Baykov, B. Johansson, V. V. Dmitriev, and M. S. Blanter, “Oxygen and nitrogen interstitial ordering in hcp Ti, Zr, and Hf: An ab initio study,” *Phys. Rev. B*, vol. 82, no. 134110, pp. 1–10, Oct. 2010.

[11] R. A. Assink and R. W. Schwartz, “H and C NMR Investigations of Pb(Zr,Ti)O3 Thin-Film Precursor Solutions,” *Chem. Mater.*, vol. 5, no. 15, pp. 511–517, 1993.

[12] T. Maeder, L. Sagalowicz, and P. Muralt, “Stabilized Platinum Electrodes for Ferroelectric Film Deposition using Ti , Ta and Zr Adhesion Layers,” *Jpn. J. Appl. Phys.*, vol. 37, pp. 2007–2012, 1998.

[13] F. K. Lotgering, “Topotactical reactions with ferrimagnetic oxides having hexagonal crystal structures. I,” *J. Inorg. Nucl. Chem.*, vol. 9, no. 2, p. 113–, 1959.

[14] Y. Bastani, T. Schmitz-Kempen, A. Roelofs, and N. Bassiri-Gharb, “Critical thickness for extrinsic contributions to the dielectric and piezoelectric response in lead zirconate titanate ultrathin films,” *J. Appl. Phys.*, vol. 109, no. 1, p. 014115, 2011.